Beam-plasma instability in charged plasma in the absence of ions

Alexander E. Dubinov, Alexey G. Petrik, Semen A. Kurkin, Nikita S. Frolov, Alexey A. Koronovskii, and Alexander E. Hramov'

Citation: Physics of Plasmas **23**, 042105 (2016); doi: 10.1063/1.4945644
View online: http://dx.doi.org/10.1063/1.4945644
View Table of Contents: http://aip.scitation.org/toc/php/23/4
Published by the American Institute of Physics

PHYSICS OF PLASMAS **23**, 042105 (2016)

Beam-plasma instability in charged plasma in the absence of ions

Alexander E. Dubinov,[1] Alexey G. Petrik,[2] Semen A. Kurkin,[2,3] Nikita S. Frolov,[2,3] Alexey A. Koronovskii,[2,3] and Alexander E. Hramov[2,3,a)]
[1]*National Research Nuclear University "MEPhI," Kashirskoe Highway, 31, Moscow 115409, Russia and Sarov State Institute of Physics and Technology (SarFTI) of National Research Nuclear University "MEPhI," Dukhova Str., 6, Sarov, Nizhni Novgorod Region 607186, Russia*
[2]*Saratov State Technical University, Politechnicheskaja 77, Saratov 410028, Russia*
[3]*Saratov State University, Astrakhanskaja 83, Saratov 410012, Russia*

(Received 17 February 2016; accepted 24 March 2016; published online 8 April 2016)

We report on the possibility of the beam-plasma instability development in the system with electron beam interacting with the single-component hot electron plasma without ions. As considered system, we analyse the interaction of the low-current relativistic electron beam (REB) with squeezed state in the high-current REB formed in the relativistic magnetically insulated two-section vircator drift space. The numerical analysis is provided by means of 3D electromagnetic simulation in CST Particle Studio. We have conducted an extensive study of characteristic regimes of REB dynamics determined by the beam-plasma instability development in the absence of ions. As a result, the dependencies of instability increment and wavelength on the REB current value have been obtained. The considered process brings the new mechanism of controlled microwave amplification and generation to the device with a virtual cathode. This mechanism is similar to the action of the beam-plasma amplifiers and oscillators. © *2016 AIP Publishing LLC*.
[http://dx.doi.org/10.1063/1.4945644]

I. INTRODUCTION

The beam-plasma instability is the fundamental dynamical process, which was discovered in 1949 independently by Akhiezer and Fainberg[1] as well as by Bohm and Gross.[2] A large number of works deal with investigations and numerous applications of the beam-plasma instability. It consists in the excitation of longitudinal electron oscillations in the plasma when electron beam is passed through it. The beam-plasma instability is used in the beam-plasma microwave generators and amplifiers[3–5] and for the excitation of the beam-plasma discharges for application in technologies.[6,7]

The beam-plasma instability increment in the linear stage is proportional to the derivative of the electron velocity distribution function at the point of synchronism between the wave and electrons of the beam. The quasi-linear theory of the interaction built in Refs. 8–10 reveals the evolutionary process of the total distribution function of beam and plasma electrons during the instability development: the gap between the maxima in the total distribution function that corresponds to beam and plasma electrons is gradually smoothed by the diffusion. Strongly turbulent state is established in plasma on the nonlinear stage of the beam-plasma instability development, and the solitary coherent structures such as solitons[11] or phase vortices[12] are generated in the system. The results of theoretical and numerical analysis of all stages of the beam-plasma instability development are presented in the comprehensive reviews.[13,14]

The stationary ion background providing quasi-neutrality of beam-plasma system and occurrence of the restoring force acting on the plasma electrons deflected from the equilibrium position is believed to be required for the beam-plasma instability development. There is an important question, whether it develops the beam-plasma instability in the case, when electron beam is interacting with the stationary single-component hot electron plasma without ions, for example, confined in a trap or created in a some other way? And what are the features of the beam-plasma instability in such system? Hitherto, these questions remained unanswered.

The goal of this work is the particle-in-cell (PIC) simulation of the beam-plasma instability development in the system with electron beam interacting with the single-component hot electron plasma without ions. The so-called squeezed state of electron beam was chosen as such plasma. For the first time, the squeezed state of electron beam was discovered in the magnetically insulated two-section vircators.[15] The phenomenon of squeezed state of electron beam consists in the following. At the initial stage of the squeezed state formation, immediately after the beginning of the reflections of electrons from the virtual cathode (VC), two-beam state of the counter-propagating electron beams is established in the potential well between the real and virtual cathodes. It is known that the counter-propagating electron beams cannot be in the unperturbed state for a long time because the excitation of various beam instabilities, in particular, the two-beam instability, is possible in such system. However, it turned out that in counter-propagating beams with current exceeding the space-charge-limited current there is the faster instability than the two-beam one. This instability leads to the formation of a dense hot cloud of charged electron plasma characterized by a high density of electrons and fully developed turbulence. In fact, the squeezed state of electron beam represents a distributed in the drift space virtual cathode that can be examined on the

[a)]Electronic mail: hramovae@gmail.com

specific profile of the electron beam phase portrait when the counter-propagating beams are closed up along the longitudinal velocity axis and form the region of strongly heated electron cloud. The process of the squeezed state establishment has a kind of longitudinal switching wave: "the two-beam state switches to the squeezed state" and is accompanied by an additional electric charge accumulation, and the switching wave velocity is defined by the rate of the charge accumulation. Later, the squeezed state of electron beam has been found out in the vircator with counter-propagating beams,[16] electronic traps,[17–21] in the laser plasma.[22] Different aspects of dynamics of the squeezed state of electron beam in various high-power microwave devices have been investigated in Refs. 21 and 23–31. It is proposed in Refs. 32 and 33 to use squeezed state of electron beam for collective ion acceleration and in Ref. 34—to gain a beam discharge.

In this paper, the possibility of the beam-plasma instability development in squeezed state in the intense relativistic electron beam (REB) with the use of additional low-current electron beam in the relativistic magnetically insulated vircator has been shown for the first time with the help of PIC-simulation in CST Particle Studio. The considered process brings the new mechanism of controlled microwave amplification and generation to the device with a virtual cathode. This mechanism is similar to the action of the beam-plasma amplifiers and oscillators. The structure of the paper is the following. In Section II, we briefly describe the proposed numerical model. In Section III, a systematic numerical analysis is carried out, based on a model of two beam propagation in the two-section drift space. In Section IV, the characteristics of beam-plasma instability with absence of ions are investigated. Conclusions are drawn in Section V.

II. SYSTEM UNDER STUDY

Analyzing relativistic electron beams (REBs), it is necessary to take into account effects being insignificant for the weakly relativistic systems, in particular, the influence of the self-magnetic field of a REB. The simultaneous coexistence of two instabilities in a REB resulting in formation of squeezed state and beam-plasma instability leads to the complex beam dynamics in the system that may be efficiently analyzed mainly with the help of the numerical methods based on the solving of the self-consistent system of Maxwell equations and motion equations of charged particles. For that reason, the three-dimensional fully electromagnetic self-consistent CST Particle Studio package, which has worked well in the simulation of different beam instabilities and high-power electron devices,[35–42] is used in our work for the accurate numerical investigations of physical processes in the relativistic two-section vircator model.

During our numerical treatment, we have investigated the interaction between two drifting monoenergetic REBs with different particle energy levels and inner radii R_{b1} and R_{b2} ($R_{b1} < R_{b2}$), respectively, in the vircator system illustrated in Fig. 1. Notable that the inner REB of radius R_{b1} is in the squeezed state of the electron beam and forms the active media for the instability development. The system

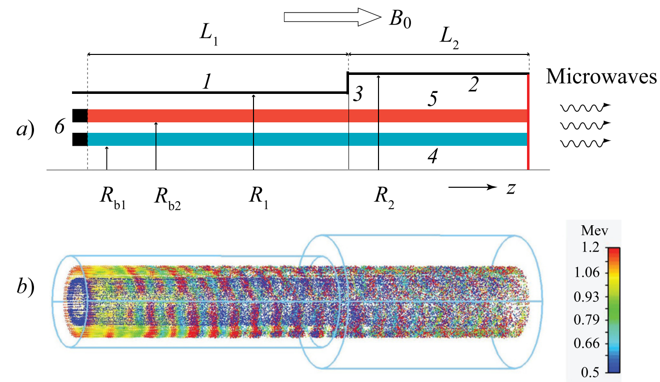

FIG. 1. Schematic illustration of system under study (a) and its realization as a 3D model in CST Particle Studio in the presence of charged particles in the regime of beam-plasma instability observation (b). Here, 1 is the first drift tube of radius R_1 and length L_1, 2 is the second drift tube of radius R_2 and length L_2, 3 is the grid electrode that divides these tubes, 4 is the inner annular REB of radius R_{b1}, beam current I_{b1}, and particles' energy U_{b1} that provides the formation of the squeezed state of REB, 5 is the additional outer annular REB of radius R_{b2}, beam current I_{b2}, and particles' energy U_{b2}, and 6 is the set of two cylindrical REB emitters.

under study, similar to the one investigated in Ref. 15, consists of two perfect electric conducting finite-length cylindrical waveguide regions (the electron beam drift chamber), marked as 1 and 2, of the different radii $R_1 = 15$ mm and $R_2 = 22$ mm and the lengths $L_1 = 88$ mm and $L_2 = 70$ mm, respectively. The thicknesses of the beams are equal to $\Delta = 2$ mm. The drift chamber 2 has a grid electrode 3 on the left side and a cylindrical waveguide port on the right side. Two cylindrical annular REBs—the inner and the outer one, denoted as 4 (blue color in online) and 5 (red color in online), are injected from the emitters 6.

We have selected DC model of REB emission during our numerical treatment with fixed beam currents, I_{b1}, I_{b2}, and fixed particle energies, U_{b1}, U_{b2}, which are different for inner and outer beams. The inner beam of radius $R_{b1} = 6$ mm, beam current $I_{b1} = 12$ kA, and beam particles' energy $U_{b1} = 0.4$ MeV is the slow one and provides the formation of the squeezed state due to the beam current value I_{b1} being in accord with the condition of squeezed state formation.[15] So the inner electron beam acts as a rather low-energy one-component plasma-like active media. The additional outer REB of radius $R_{b2} = 10$ mm, beam current $I_{b2} = 1.5$ kA, and beam particles' energy $U_{b2} = 1.2$ MeV consists of significantly faster charged particles and demonstrates stable behavior in the absence of the inner electron beam. The outer low-current electron beam is injected in the drift space with time delay $\tau = 6$ ns. As we will show later in Section III, during this time the squeezed state is formed fully in the inner high-current REB. These two beams are held by means of external homogenous in space longitudinal magnetic field $B_0 = 5$ T.

The main goal of our numerical experiment is to show and to describe the process of the instability development during the interaction of high-energy REB with the electron active media in the form of REB in the squeezed state. Further, we discuss the results of carried out numerical simulation.

III. NUMERICAL SIMULATION RESULTS

Let us start with the discussion of the squeezed state formation in the inner electron beam. The best way to illustrate this process is to plot the sequence of instant REB phase portraits in the plane "longitudinal coordinate z-longitudinal velocity v_z" (Fig. 2). It is clearly seen that the virtual cathode reflecting the electrons back to the injection area is formed in the second drift chamber at $t = 2.5$ ns (Fig. 2(b)). After that starting with $t = 2.7$ ns, the squeezed state of the electron beam is formed in the REB (Fig. 2(c)). By the time moment $t \approx 3.6$ ns, the squeezed state of the electron beam fills nearly all space of the first drift tube. If we will continue the injection of the REB with the same fixed beam current and particles' energy level, the well-formed squeezed state of the electron beam will not change and remain stable in time (see phase portrait in Fig. 2(d) plotted for $t = 4.6$ ns). The electron distribution function of this REB state corresponds to a hot single-component plasma with temperature close to 50 keV.

Afterwards, when the stable squeezed state is set in the inner REB, the additional outer low-current REB is injected (6 ns after the inner high-current REB injection). We suggest that the particles' energy of the outer REB is high in comparison with the particles of the REB in squeezed state and equals 1.2 MeV. Fig. 3 shows the temporal evolution of inner and outer REBs' phase portrait. One can see that at the early time the double-beam system demonstrates the slightly

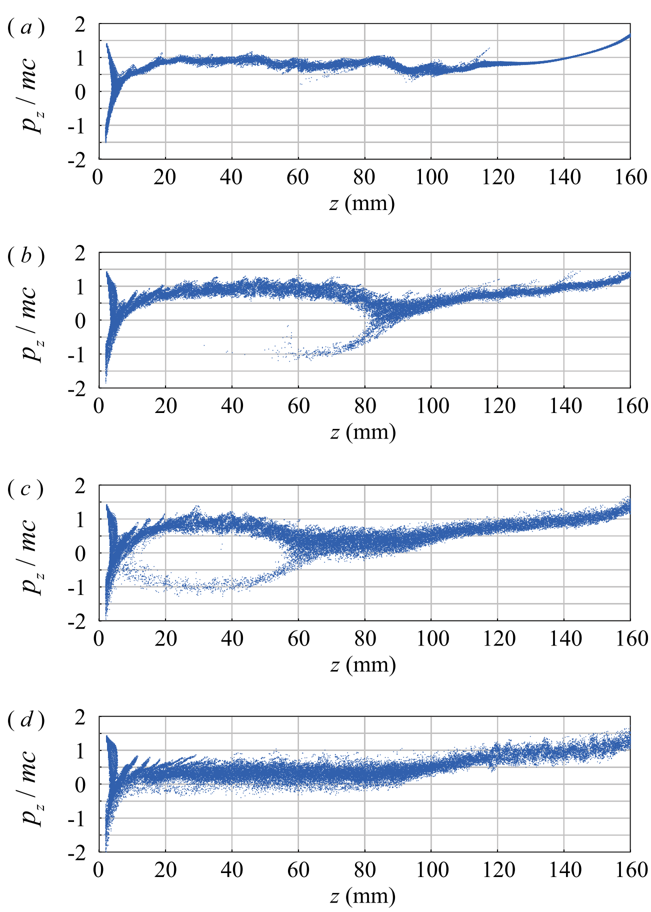

FIG. 2. Sequence of the inner annular REB phase portraits in the coordinates (z, v_z) that shows the temporal evolution of the squeezed state of the REB: (a) $t = 1.2$ ns, (b) $t = 2.5$ ns, (c) $t = 3.1$ ns, and (d) $t = 4.6$ ns.

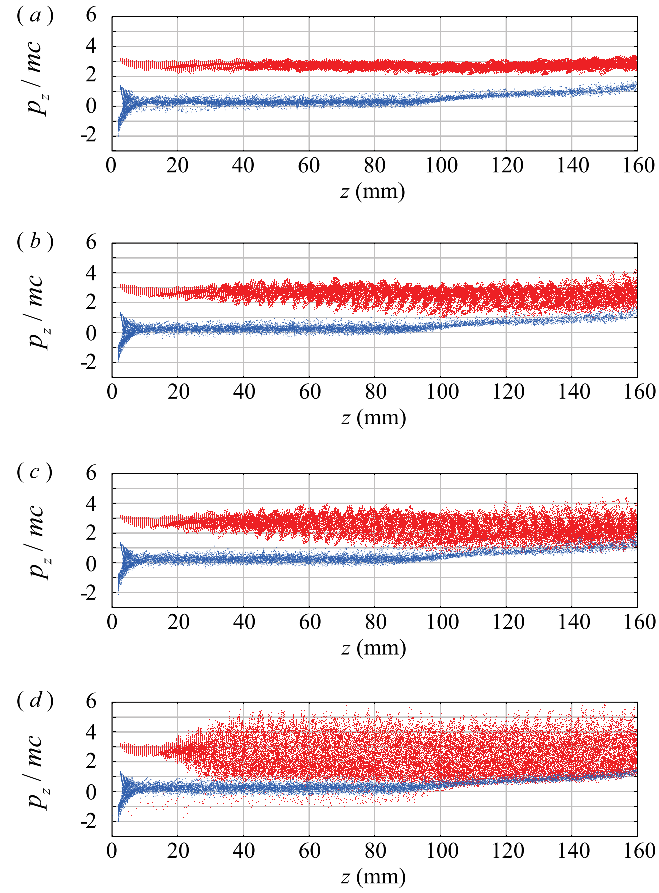

FIG. 3. Sequence of the annular REBs' phase portraits in the coordinates (z, v_z) in the case of two beams in the system: the inner REB, where the squeezed state is formed (blue points in online version), and the additional outer REB (red points in online version). These phase portraits illustrate the dynamics of the beam-plasma instability development in the absence of ions at the different time moments: (a) $t = 7.1$ ns, (b) $t = 8.4$ ns, (c) $t = 9.3$ ns, and (d) $t = 22$ ns.

disturbed state according to the phase portrait in Fig. 3(a). Then, the beam-plasma instability starts to arise (Fig. 3(b)). This instability belongs to the convective type and leads to the excitation of the longitudinal helical space-charge wave in the outer high-energy electron beam (see Figs. 1(b) and 3(c)). Such wave structure is determined by instability of the helical space-charge mode in a cylindrical electron beam in the external longitudinal magnetic field (see, e.g., Ref. 43). Actually, if we consider the initial perturbation of the space-charge in the outer beam in the form of a helix, then the azimuthal Lorentz force acting on the electrons outside the perturbation will force them to move in the direction of the nearest space-charge maximum. So the helical perturbation will grow.

The analysis of space-charge density behavior shows that the excited space-charge waves in the outer REB differ from those in the REB in squeezed state (compare Figs. 4(a) and 4(b)). The instability forces the formation and drift of the fast and high-frequency electron groups in the additional outer REB and much slower ones—in the inner REB—with significantly less frequency. Note that the evolution of the concerned beam-plasma instability in the absence of ions is a rather rapid process. After a few nanoseconds, we observe

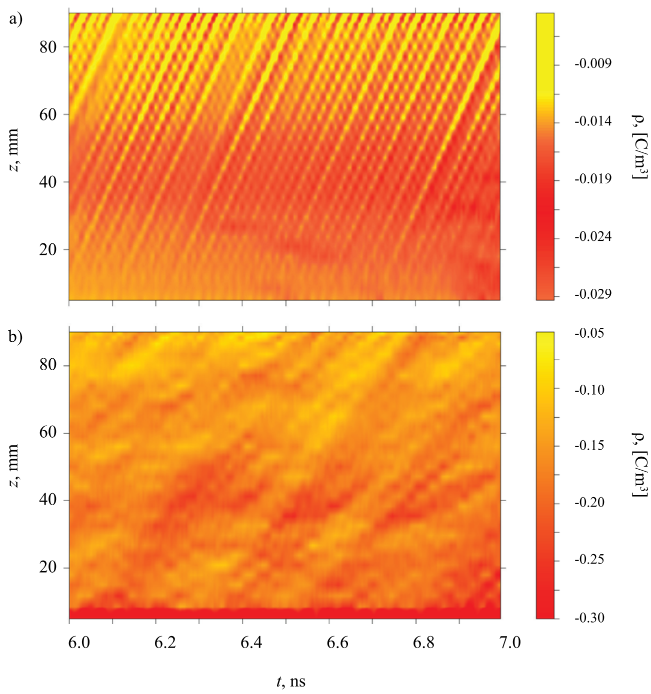

FIG. 4. Spatio-temporal behavior of space-charge in the additional outer REB (a) and in the inner beam in the squeezed state (b).

the well-pronounced breakdown of the spatial space-charge oscillations, and then we observe the developed noise-like beam-plasma oscillations (in the considered case, the time between the start of the oscillations and the breakdown is approximately 14 ns) (Fig. 3(d)).

The temporal evolution of the electron distribution function, that takes into account the charged particles of both inner REB in squeezed state and additional outer REB, shows interesting details referring to the beam-plasma instability development. The observed distribution function is presented in Fig. 5. One can see that the processes, taking place in the studied beam-plasma system in the absence of ions, lead to smoothing of the gap between the two peaks (marked by the arrows in Fig. 5), corresponding to the squeezed state and the additional outer REB. Such behavior of the distribution function is inherent to the process of electron beam relaxation during the beam-plasma instability development in the electron-ionic plasmas.[44,45]

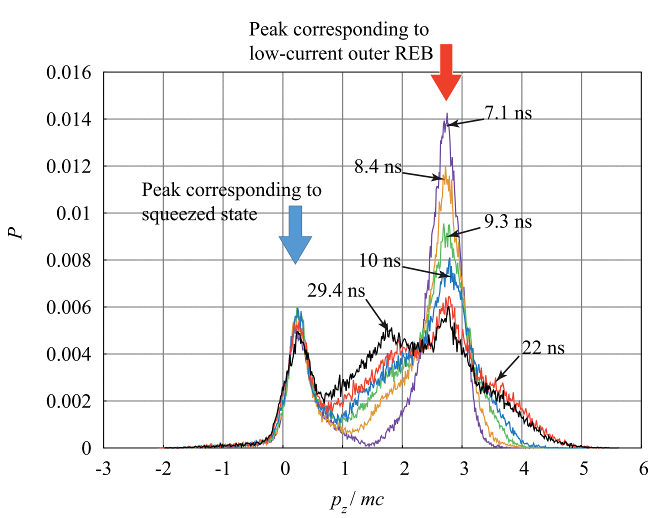

FIG. 5. The electron distribution functions including both the additional outer REB and the inner REB in the squeezed state for different time moments.

IV. CHARACTERISTICS OF BEAM-PLASMA INSTABILITY WITH ABSENCE OF IONS

As the observed beam-plasma instability leads to the formation of the longitudinal helical space-charge waves, we are able to analyze the phase portraits and the space-charge distributions and estimate important characteristics of disturbed beam dynamics, such as spatial instability increment and wavelength of the excited spatial oscillations. We have shown that the characteristic spatial scale of the excited space-charge waves lies in the millimeter range of wavelengths (see Fig. 6). We have also studied the dependence of the spatial instability increment and wavelength of the excited wave on the outer beam current value. The spatial increment of the observed beam-plasma instability grows with the increase of beam current *I* of the additional outer REB, while the wavelength of the excited space-charge waves decreases.

We have also carried out the spectral analysis of the space-charge waves in the both interacting REBs to define main oscillations' frequencies of charged particles' groups, excited by the instability. Without the additional outer REB, the power spectrum of the space-charge oscillations in squeezed state and the spectrum of output microwave radiation lie in 1–5 GHz frequency range. We have also calculated the power spectrum of the space-charge oscillations from 0.5 to 50 GHz and considered two main cases of additional outer REB dynamics. (i) We have considered the dynamics of the additional outer REB in the absence of the inner REB in squeezed state. (ii) We have analyzed the non-stationary behavior of the outer REB in the presence of the inner REB in squeezed state. We have obtained that the additional outer REB does not demonstrate the oscillations in the 30–50 GHz range in the absence of inner REB in the regime of the squeezed state formation. In the case of inner beam current $I_{b1} = 12$ kA, we have only observed high-power oscillations in the low-frequency 1.8–4.2 GHz range. At the same time, the injection of the additional outer REB in the case, when the inner beam is in the squeezed state, leads to the appearance of high-frequency oscillations, characterized by two

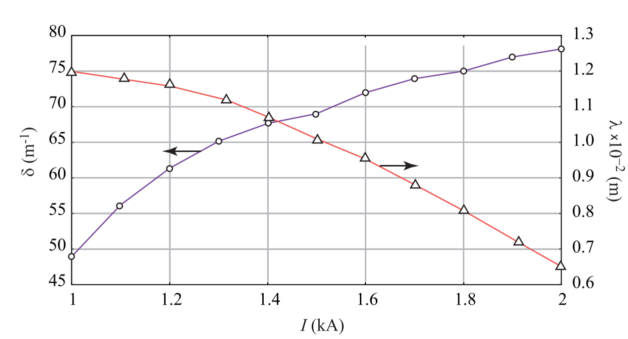

FIG. 6. The dependencies of the instability increment (○) and the space-charge oscillations' wavelength (△) on the outer REB current value *I* that were obtained on the linear stage of the instability development.

main peaks in the power spectrum with the frequencies 36.8 GHz and 40.1 GHz for $I_{b1} = 12$ kA and $I_{b2} = 1.5$ kA. Note that the same peaks are observed in the power spectrum of the space-charge oscillations registered in the region of inner REB in squeezed state. With increasing beam currents I_{b1} and I_{b2}, we have observed the increase of typical frequencies of oscillations in the additional outer beam. So, for the inner beam current $I_{b1} = 12$ kA and the additional beam current $I_{b2} = 3.0$ kA, the maximal oscillation frequency is 44.7 GHz; for $I_{b2} = 8.0$ kA–52.6 GHz. At the same time, in the case of large beam current I_{b2}, we have observed the complex nonlinear dynamics of the additional beam space charge characterized by complex power spectra with many additional peaks in 39.2–52.6 GHz frequency range. Such regimes require further investigations. It should be noted that the further increase of the beam current leads to the destruction of the squeezed state due to the virtual cathode formation already in the first drift tube with a smaller radius; therefore, there is the necessity to reduce the radii of the drift tubes of two-section vircator to increase the space-charge-limited current.

The fact that the observed beam-plasma instability leads to the excitation of high-frequency oscillations in the additional outer REB gives the background to the creation of the concepts and techniques for significant increasing the frequency of high-power electromagnetic signals' generation and amplification based on the investigated effect of beam—plasma without ions' interaction.

V. CONCLUSION

We have shown for the first time the possibility of the beam-plasma instability development in the system with electron beam interacting with the single-component hot electron plasma without ions. To realize such electron plasma without ions, we have used the idea of the formation of squeezed state of relativistic electron beam in the magnetically insulated two-section vircator. The obtained results of 3D numerical simulation by means of CST Particle Studio software reveal the basic features of the development and interaction of Bursian instability, leading to the squeezed state formation and beam-plasma instabilities in the nonneutral REB. It has been found out that the beam-plasma instability in the considered two-section vircator system with the two tubular beams is developed and leads to space-charge oscillations in the additional relativistic electron beam. For the first time, the important feature of the development of the beam-plasma instability in the single-component hot electron plasma without ions has been found out in the present work numerically. Nevertheless, this significant effect requires further more detailed studies, particularly, the formulation of the analytical or semi-analytical theory of such kind of the beam-plasma instability.

Due to the generality of the considered model, the obtained results have additional interest because they may be used for the significant increase of the frequency of microwave signals' generation and amplification in the devices of high-power microwave electronics.

ACKNOWLEDGMENTS

The numerical studies of the development of beam-plasma instability of REB dynamics have been supported by the Russian Science Foundation (Grant No. 14-12-00222). N.S.F. acknowledges individual financial support from the Russian Foundation for Basic Research (Grant No. 16-32-60107).

[1]A. I. Akhiezer and Y. Fainberg, "High-frequency oscillations of an electron plasma," Dokl. Akad. Nauk SSSR **64**, 555 (1949).
[2]D. Bohm and E. P. Gross, "Theory of plasma oscillations. B. Excitation and damping of oscillations," Phys. Rev. **75**, 1864–1876 (1949).
[3]L. S. Bogdankevich, M. V. Kuzelev, and A. A. Rukhadze, "Plasma microwave electronics," Sov. Phys. Usp. **24**, 1 (1981).
[4]M. V. Kuzelev, F. Mukhametzyanov, M. S. Rabinovich, A. A. Rukhadze, P. S. Strelkov, and A. G. Shkvarunets, "Relativistic plasma microwave oscillator," JETP **56**, 780–785 (1982).
[5]I. L. Bogdankevich, I. E. Ivanov, and P. S. Strelkov, "Experimental study and numerical simulations of a plasma relativistic microwave amplifier," Plasma Phys. Rep. **36**, 762–771 (2010).
[6]A. K. Berezin, Y. Fainberg, G. P. Berezin, L. I. Bolotin, and V. G. Stupak, "Interaction of intense electron beams with a plasma," Sov. J. At. Energy **11**, 1143–1147 (1962).
[7]S. G. Walton, C. Muratore, D. Leonhardt, R. F. Fernsler, D. D. Blackwell, and R. A. Meger, "Electron-beam-generated plasmas for materials processing," Surf. Coat. Technol. **186**, 40–46 (2004).
[8]Y. Romanov and G. F. Filippov, "The interaction of fast electron beams with longitudinal plasma waves," Sov. Phys. JETP **13**, 87–92 (1961).
[9]A. A. Vedenov, E. P. Velikhov, and R. Z. Sagdeev, "Stability of plasma," Sov. Phys. Usp. **4**, 332–369 (1961).
[10]V. D. Shapiro and V. I. Shevchenko, "Quasilinear theory of relaxation of an electron beam in a magnetoactive plasma," Sov. Phys. JETP **27**, 635–642 (1968).
[11]V. D. Fedorchenko, Y. Mazalov, A. S. Bakai, A. V. Pashenko, and B. N. Rutkevich, "Excitation of solitary waves in a beam-plasma system," JETP Lett. **18**, 281–282 (1973).
[12]B. Eliasson, P. K. Shukla, and M. E. Dieckmann, "Theory and simulations of nonlinear kinetic structures in plasmas," Plasma Phys. Controlled Fusion **48**, 257–265 (2006).
[13]P. C. Jagher de, F. W. Sluijter, and H. J. Hopman, "Relativistic electron beams and beam-plasma interaction," Phys. Rep. **167**, 177–239 (1988).
[14]A. Bret, L. Gremillet, and M. E. Dieckmann, "Multidimensional electron beam-plasma instabilities in the relativistic regime," Phys. Plasmas **17**, 120501-1–120501-36 (2010).
[15]A. M. Ignatov and V. P. Tarakanov, "Squeezed state of high-current electron beam," Phys. Plasmas **1**, 741–744 (1994).
[16]A. E. Dubinov, I. A. Efimova, Y. I. Kornilova, S. K. Saikov, V. D. Selemir, and V. P. Tarakanov, "Nonlinear dynamics of electron beams with a virtual cathode," Phys. Part. Nucl. **35**, 251–284 (2004).
[17]G. Bettega, F. Cavaliere, M. Cavenago, A. Illiberi, R. Pozzoli, and M. Rome, "Experimental and numerical analysis of the electron injection in a Malmberg-Penning trap," Phys. Plasmas **14**, 042104 (2007).
[18]E. D. Donets, E. E. Donets, E. M. Syresin, A. E. Dubinov, I. V. Makarov, S. A. Sadovoy, S. K. Saikov, and V. P. Tarakanov, "Formation of longitudinal nonlinear structures in the electron cloud of an electron-string ion source," Plasma Phys. Rep. **35**, 54–61 (2009).
[19]E. D. Donets, E. E. Donets, E. M. Syresin, A. E. Dubinov, I. V. Makarov, S. A. Sadovoi, S. K. Saikov, and V. P. Tarakanov, "Nonlinear dynamics of longitudinal structures in the electron cloud of a coaxial electron string ion source," Tech. Phys. **56**, 690–696 (2011).
[20]A. E. Dubinov, I. V. Makarov, S. A. Sadovoi, S. K. Saikov, and V. P. Tarakanov, "Specific features of accumulating electrons in high-current trap," Tech. Phys. Lett. **37**, 230–232 (2011).
[21]E. N. Egorov, A. A. Koronovskii, S. A. Kurkin, and A. E. Hramov, "Formation and nonlinear dynamics of the squeezed state of a helical electron beam with additional deceleration," Plasma Phys. Rep. **39**, 925–935 (2013).
[22]F. Fiuza, A. Stockem, E. Boella, R. A. Fonseca, L. O. Silva, D. Haberberger, S. Tochitsky, W. B. Mori, and C. Joshi, "Ion acceleration from laser-driven electrostatic shocks," Phys. Plasmas **20**, 056304 (2013).

[23]A. E. Dubinov, "Scenario for the establishment of an electron beam 'squeezed state' in a magnetically insulated vircator," Tech. Phys. Lett. **23**, 870–871 (1997).
[24]A. E. Dubinov, "Features of electron dynamics in a vircator with a magnetic mirror," J. Commun. Technol. Electron. **45**, 792–796 (2000).
[25]A. E. Dubinov and I. A. Efimova, "Dynamics of a magnetized relativistic electron beam in composite drift tubes with virtual cathodes," Tech. Phys. **46**, 723–728 (2001).
[26]S. Belomyttsev, A. A. Grishkov, S. D. Korovin, and V. V. Ryzhov, "The virtual cathode velocity during electron beam transport in a drift tube," Tech. Phys. Lett. **30**, 1060–1063 (2004).
[27]S. Belomyttsev, A. A. Grishkov, S. A. Kitsanov, S. D. Korovin, S. D. Polevin, V. V. Ryzhov, and A. P. Yachnyi, "Experimental investigation of electron beam in the squeezed state," Tech. Phys. Lett. **31**, 982–985 (2005).
[28]S. Belomyttsev, A. A. Grishkov, S. A. Kitsanov, I. K. Kurkan, S. D. Polevin, V. V. Ryzhov, and R. V. Tsygankov, "Measuring the virtual cathode velocity," Tech. Phys. Lett. **34**, 546–548 (2008).
[29]E. N. Egorov, A. A. Koronovskii, S. A. Kurkin, and A. E. Hramov, "Emerging compressed states of a spiral electron stream in a system with deceleration," Tech. Phys. Lett. **39**, 874–877 (2013).
[30]A. A. Grishkov and I. V. Pegel, "An annular high-current electron beam with an energy spread in a coaxial magnetically insulated diode," Plasma Phys. Rep. **39**, 936–946 (2013).
[31]S. Belomyttsev, A. A. Grishkov, I. K. Kurkan, and R. V. Tsygankov, "Motion of a virtual cathode in a cylindrical channel with electron beam transport in the 'compressed' state," Phys. Plasmas **21**, 033102 (2014).
[32]A. E. Dubinov, V. D. Selemir, and V. P. Tarakanov, "On the possibility of a collective acceleration of ions in a magnetically insulated vircator in the regime of a traveling distributed virtual cathode boundary," Tech. Phys. Lett. **28**, 159–161 (2002).
[33]A. E. Dubinov, Y. I. Kornilova, and V. D. Selemir, "Collective ion acceleration in systems with a virtual cathode," Phys. - Usp. **45**, 1109–1129 (2002).
[34]V. N. Barabanov, A. E. Dubinov, M. V. Loiko, S. K. Saikov, V. D. Selemir, and V. P. Tarakanov, "Beam discharge excited by distributed virtual cathode," Plasma Phys. Rep. **38**, 169–178 (2012).
[35]S. A. Kurkin, A. A. Badarin, A. A. Koronovskii, and A. E. Hramov, "The development and interaction of instabilities in intense relativistic electron beams," Phys. Plasmas **22**, 122110 (2015).
[36]S. A. Kurkin, N. S. Frolov, A. O. Rak, A. A. Koronovskii, A. A. Kuraev, and A. E. Hramov, "High-power microwave amplifier based on overcritical relativistic electron beam without external magnetic field," Appl. Phys. Lett. **106**, 153503 (2015).
[37]S. A. Kurkin, A. A. Koronovskii, A. E. Hramov, and A. O. Rak, "Optimization of the double-gap vircator with electromagnetic feedback in CST Particle Studio," in *IEEE International Vacuum Electronics Conference* (2014), pp. 389–390.
[38]M. Einat, M. Pilossof, R. Ben-Moshe, H. Hirshbein, and D. Borodin, "95 GHz gyrotron with ferroelectric cathode," Phys. Rev. Lett. **109**, 185101 (2012).
[39]M. C. Balk, "Simulation possibilities of vacuum electronic devices with CST Particle Studio," in *IEEE International Vacuum Electronics Conference, 2008 (IVEC-2008)* (2008), pp. 459–460.
[40]S. A. Kurkin, A. E. Hramov, and A. A. Koronovskii, "Microwave radiation power of relativistic electron beam with virtual cathode in the external magnetic field," Appl. Phys. Lett. **103**, 043507 (2013).
[41]S. A. Kurkin, A. A. Badarin, A. A. Koronovskii, and A. E. Hramov, "Higher harmonics generation in relativistic electron beam with virtual cathode," Phys. Plasmas **21**, 093105 (2014).
[42]A. E. Hramov, S. A. Kurkin, A. A. Koronovskii, and A. E. Filatova, "Effect of self-magnetic fields on the nonlinear dynamics of relativistic electron beam with virtual cathode," Phys. Plasmas **19**, 112101 (2012).
[43]J. A. Rome and R. J. Briggs, "Stability of sheared electron flow," Phys. Fluids **15**, 796–804 (1972).
[44]V. P. Tarakanov and E. G. Shustin, "Dynamics of beam instability in a finite plasma volume: Numerical experiment," Plasma Phys. Rep. **33**, 130–137 (2007).
[45]H. Ratcliffe, C. S. Brady, M. B. Che Rozenan, and V. M. Nakariakov, "A comparison of weak-turbulence and particle-in-cell simulations of weak electron-beam plasma interaction," Phys. Plasmas **21**, 122104 (2014).